N-linked oligosaccharides play a role in disulphide-dependent dimerization of intestinal mucin Muc2

Sherilyn L. BELL*, Gongqiao XU*, Ismat A. KHATRI*, Rongquan WANG†, Sameera RAHMAN* and Janet F. FORSTNER*[1]

*Division of Structural Biology & Biochemistry, Research Institute, The Hospital for Sick Children and the University of Toronto, 555 University Avenue, Toronto, ON M5G 1X8, Canada, and †Department of Gastroenterology, Southwestern Hospital, Chongqing, People's Republic of China, 400038

Within the C-terminal domain of many secretory mucins is a 'cystine knot' (CK), which is needed for dimer formation in the endoplasmic reticulum. Previous studies indicate that in addition to an unpaired cysteine, the three intramolecular cystine bonds of the knot are important for stability of the dimers formed by rat intestinal mucin Muc2. The present study was undertaken to determine whether the two N-glycans N9 and N10, located near the first and second cysteines of the knot, also play a role in dimer formation. The C-terminal domain of rat Muc2 (RMC), a truncated RMC mutant containing the CK, and mutants lacking N9 and N10 sites, were expressed in COS-1 cells and the products monitored by radioactive [^{35}S]Met/Cys metabolic pulse–chase and immunoprecipitation. Mutation of N9, but not N10, caused increased synthesis of dimers over a 2-h chase period. The N9 mutant remained associated with calreticulin for a prolonged period. About 34–38 % of the total labelled products of RMC and its mutants was secreted into the media by 2 h, but the proportion in dimer form was dramatically reduced for the N9 mutant, suggesting lower dimer stability relative to RMC or its N10 mutant. We conclude that under normal conditions the presence of the N9 glycan functions to maintain a folding rate for mucin monomers that is sufficiently slow to allow structural maturation and stability of Muc2 dimers. To our knowledge this report is the first demonstration that a specific N-glycan plays a definitive role in mucin dimer formation.

Key words: calreticulin, dimer, mucus glycoprotein, N-glycosylation, proteasomal inhibitor.

INTRODUCTION

Located near the C-terminus of most secretory mucins is a 90–100-residue motif termed the 'cystine knot' (CK) [1–8]. The same motif is also present in diverse non-mucin proteins, and has a conserved and distinguishing arrangement of cysteines that allows classification of the CK superfamily into growth factor, small inhibitor and cyclotide families (reviewed in [9,10]). The three-dimensional configuration of some growth factor CKs has been defined by crystallography [11–19]. The knot is maintained by three pairs of cysteines that form disulphide bonds between Cys-1 and Cys-4, Cys-2 and Cys-5, and Cys-3 and Cys-6, respectively. In the growth-factor group, the Cys-1–Cys-4 bond penetrates a ring formed by the remaining cystines, and dimers are formed through intermolecular disulphide bonds, hydrophobic interactions or both [9]. Our previous studies of rat intestinal mucin Muc2 (rMuc2) revealed that to form a dimer an unpaired cysteine (designated Cys X), adjacent to Cys-4 of the knot, bridges to the equivalent Cys X on a neighbouring molecule. In addition, however, there is an important contribution of the three internal cystine bonds, especially that involving Cys-1–Cys-4, to the structural stability and dimerization competence of the C-terminal domain [20]. Our experiments also suggested the necessity of N-glycosylation for correct maturation of the mucin domain, as treatment with tunicamycin inhibited dimer formation as well as secretion [21]. Since there are two N-glycosylation consensus sites in the vicinity of Cys-1 of the knot, the present study was undertaken to determine whether one or both of these N-glycans might specifically influence the nature, extent or rate of dimer formation and/or secretion of rMuc2.

During biosynthesis of glycoproteins, N-glycosylation is initiated co-translationally in the endoplasmic reticulum (ER), and further maturation of oligosaccharides continues throughout transport to the *trans*-Golgi [22]. The significance of N-glycosylation in mucin molecules has not received much attention, since N-glycans are in relatively low abundance and largely confined to the end regions of the molecule. The dominant glycosylation in mucins is the extensive O-linked oligosaccharide component of the centrally located tandem repeat modules. In non-mucin proteins, the role of N-glycans in processing, stability and intracellular transport has been the subject of extensive studies. N-linked glycans can influence protein folding, assembly and topology of protein complexes, developmental maturation, growth regulation, intracellular signalling, immune modulation and other important functions [23–28]. Crystallization and other structural studies have suggested that N-glycans do not affect overall conformational changes in a protein backbone. They can, however, reduce backbone flexibility and solvent access, and thereby increase stability of a protein, sometimes even in regions remote from the N-glycan-attachment sites [29,30].

N-glycans are also active participants in the maintenance of the quality-control system of cells. Trimming and reglucosylation of N-glycans ensure optimal protein interactions within the ER [31,32], as the presence of glucose influences binding of chaperones such as calnexin and calreticulin. Folding experiments in Semliki forest virus and influenza haemagglutinin, for example, have demonstrated that the position of an N-glycan on the growing peptide chain may determine which molecular chaperone is recruited for optimizing folding and stability [33].

There are indications that full-length mucins depend in some fashion upon N-glycosylation for their maturation and secretion. Treatment with tunicamycin retarded formation of higher-order oligomers in rat gastric mucin [34], intestinal MUC2 [35,36] and other secretory mucins [36]. MUC2 has also been shown to bind

Abbreviations used: CK, cystine knot; endo H, endo-β-N-acetylglucosaminidase H; ER, endoplasmic reticulum; hCG, human chorionic gonadotropin; RMC, rMuc2 C-terminal domain; rMuc2, rat intestinal mucin Muc2.

[1] To whom correspondence should be addressed (e-mail jfforst@sickkids.on.ca).

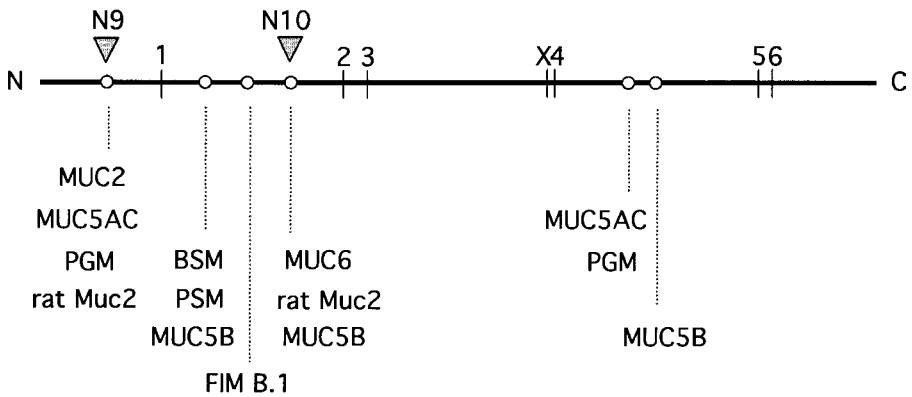

Figure 1 The CK region near the C-terminus of rMuc2 and other secretory mucins

The distance from N to C represents the C-terminal 115 amino acids of rMuc2. Numbers 1–6 refer to the six conserved cysteines of the CK. X refers to the unpaired cysteine required for intermolecular cystine-bond formation. Circles mark the approximate locations of N-glycosylation consensus sites as they occur in alignments of the secretory mucins rMuc2, human MUC2, MUC5AC, MUC5B, and bovine submaxillary mucin (BSM), porcine submaxillary mucin (PSM), porcine gastric mucin (PGM) and frog integumentary mucin B.1 (FIM-B.1). The two N-glycosylation sites in rMuc2 (N9, N10) are found -5 and $+17$ residues from Cys-1.

calreticulin [37], indicating that chaperone interaction with N-glycans is part of normal mucin maturation.

The present studies involved transient expression of the rMuc2 C-terminal domain (RMC) and mutant constructs in COS-1 cells under radioactive pulse and metabolic chase conditions. Results suggest that a specific N-glycan associated with the CK of rMuc2 alters the kinetics and structural integrity of the dimer. Since early dimer formation is the first step in the complex chain of polymerization and gel formation of secretory mucins, identification of regulatory steps affecting dimerization is an important goal. From this knowledge new opportunities may arise for altering mucin production in diseases involving mucins, such as adenocarcinoma, asthma, cystic fibrosis, epithelial infection and inflammation.

EXPERIMENTAL

Mutation of N-glycosylation sites in the vicinity of the CK

Constructs were generated using pRMC and pCK as templates. These constructs, and use of the expression vector pSVL, have been described in earlier publications [20,21]. Construct pRMC encodes the signal peptide, a three-residue linker, and the C-terminal 534 amino acids of rMuc2, which include 10 potential N-glycan sites and the CK. Construct pCK encodes the signal peptide, linker and the C-terminal 115 amino acids of rMuc2, which includes the N9 and N10 consensus sites and the CK (Figure 1). Near the 5′-end of each construct is a sequence designated D4553, which is a rMuc2 epitope used earlier to develop a synthetic peptide and a corresponding polyclonal antibody [38]. N9 and N10 are located -5 and $+17$ residues respectively from the first cysteine (Cys-1) of the CK motif (Figure 1). Analogous N-glycan sites occur in several other secretory mucins. N9 and N10 consensus sites in both RMC and CK were mutated to alanine using the QuikChange site-directed mutagenesis kit (Stratagene, La Jolla, CA, U.S.A.). The altered sites were designated N9A and N10A, or N9A/N10A in double mutants.

For mutation of N9 to alanine in pRMC, complementary DNA primers, 5′-CATGCATCCATAACCCTGCCAACACAGTCCCTTGCT-3′ (sense) and 5′-AGCAAGGGACTGTGTTGGCAGGGTTATGGATGCATG-3′ (antisense), were used. To mutate the N10 site, the primers 5′-CAATGGCTGCGCCAAGGCCATCTCCATGAACTTCTG-3′ (sense) and 5′-CAGAAGTTCATGGAGATGGCCTTGGCGCAGCCATTG-3′ (antisense) were used. All primers were synthesized by the Centre for Applied Genomics, The Hospital for Sick Children, Toronto, ON, Canada. The constructs were named pRMC-N9A and pRMC-N10A, respectively. Site-specific mutagenesis was also performed on pRMC-N9A using N10A primers to generate the double mutant lacking both N9 and N10 (pRMC-N9/10A). Primers 5′-ACTGTATCCATAACCCTGCCAACACAGTCCCTT-3′ (sense) and 5′-AAGGGACTGTGTTGGCAGGGTTATGGATACAGT-3′ (antisense) were used to mutate N9 in the construct pCK. The N10 site was mutated using the same N10A primer set shown for pRMC above. The resulting constructs were called pCK-N9A and pCK-N10A, respectively. All mutations were confirmed by sequencing in both directions.

Cell culture and immunoprecipitation

COS-1 cells (CRL-1650; ATCC) were cultured in Dulbecco's modified Eagle's medium supplemented with penicillin (100 units/ml), streptomycin (100 μg/ml) and 10 % fetal bovine serum (Invitrogen, Carlsbad, CA, U.S.A.) at 37 °C with 5 % CO_2. Transfections were performed as described previously [20] using LipofectAmine followed by a 48-h incubation in OptiMem (both from Invitrogen). After starving the cells for 30 min in Dulbecco's modified Eagle's medium deficient in cysteine and methionine, radioactive pulse–chase studies were done with ^{35}S Pro-mix *in vitro* Met/Cys cell-labelling mix (Amersham Biosciences Canada, Oakville, ON, Canada). Pulse and chase times varied as described in the appropriate Figure legends. Translation products were immunoprecipitated with anti-D4553 (anti-rMuc2) antibody as described previously [20]. In some experiments precipitation was carried out with anti-calreticulin antibody (Affinity Bioreagents, Golden, CO, U.S.A.). For these experiments the stock antibody (4 μl) was incubated for 1 h with lysates that had been precleared with 4 μl of rabbit preimmune serum complexed to Protein A–agarose. The anti-calreticulin antibody–antigen complexes were then precipitated with 50 μl of Protein A–agarose, washed twice with RIPA buffer, then once with 10 mM Tris/HCl, pH 7.5, containing 0.1 % Nonidet P-40. The samples were then suspended in 60 μl of Laemmli sample buffer for SDS/PAGE.

Proteasomal inhibition experiments involved similar pulse–chase experiments in the presence or absence of 10 μM clasto-lactacystin β-lactone (Sigma-Aldrich, St. Louis, MO, U.S.A.). The β-lactone was dissolved in DMSO, added 1 h prior to the pulse and maintained during the 15-min pulse and 2-h chase periods. The equivalent amount of DMSO (1 %) alone was added to control incubations, which gave results that were indistinguishable from untreated samples (results not shown). The lysates were immunoprecipitated as usual with anti-D4553 antibody before SDS/PAGE.

In separate experiments, RMC translation products were tested for sensitivity to endo-β-N-acetylglucosaminidase H (endo H; EC 3.2.1.96; New England BioLabs, Beverly, MA, U.S.A.) by incubation of radiolabelled immunoprecipitated cell proteins with 50 units of enzyme in a total volume of 35 μl according to the manufacturer's instructions. Endo H sensitivity was detected by a mobility shift of RMC during SDS/PAGE of immunoprecipitates [39].

SDS/PAGE

Suspensions of immunoprecipitates were divided in two, boiled for 3 min with or without the addition of dithiothreitol (final concentration 10 mM), and the products separated by SDS/PAGE (4–12 % gels) at 125 V unless noted otherwise. Gels were fixed for 10 min (30 % methanol/10 % acetic acid, v/v), dried and exposed to Kodak Biomax MR film. Autoradiograms were scanned digitally with the FluorChem 8000™ imaging system and bands were quantified using AlphaEase™ (both from Alpha Innotech Corporation, San Leandro, CA, U.S.A.). Figures were printed using a Kodak 8600 dye-sublimation printer.

Statistical analysis

Radioactivity incorporated into total products, dimers or monomers of cell lysates or media was quantified as described above and values were compared using a two-tailed unpaired Student's t test. Differences were considered significant if P values were < 0.05. In experiments with β-lactone, results were calculated as a percentage of DMSO-treated controls (set to 100 %), and expressed as means $\pm$ 95 % confidence limits.

RESULTS

Incorporation of [^{35}S]Met/Cys into expressed products of pRMC (rMuc2 C-terminal domain) and its N-glycan mutants pRMC-N9A and pRMC-N10A

After 15 min of radioactive pulse and zero non-radioactive chase, immunoprecipitates of lysates of pRMC-transfected COS-1 cells gave rise to a dimer (approx. 165 kDa) and a small quantity of 100 kDa monomer (designated 'precursor' monomer in earlier publications [20]; Figure 2A). After thiol reduction the dimer and monomer disappeared, and the only product was the reduced monomer at about 90 kDa (Figure 2B). There were no secreted products detected at this time (results not shown). By 2 h of chase, the dimer of RMC lysates was more intense, and some of the dimer and monomer appeared in the medium. With thiol reduction, the medium products of RMC collapsed to give a single reduced monomer band (Figure 2B). As observed and discussed in earlier studies [21], the more highly glycosylated secreted products were at positions of slightly slower mobility than those of cell lysates. Thus the RMC monomer of rMuc2 forms S–S-dependent dimers at an early stage of biosynthesis (by 15 min), and at least some of these products are secreted by 2 h. The same sequence of synthesis and secretion was reported earlier for dimers of full-length human MUC2 secreted from LS180, T84 and HT29-N2 human colonic cell lines [35]. As was true for full-length MUC2, the RMC cell-lysate products were sensitive to the enzyme endo H, in keeping with their location in the ER, whereas the secreted products were resistant, indicating that further maturation and processing had taken place before secretion (results not shown).

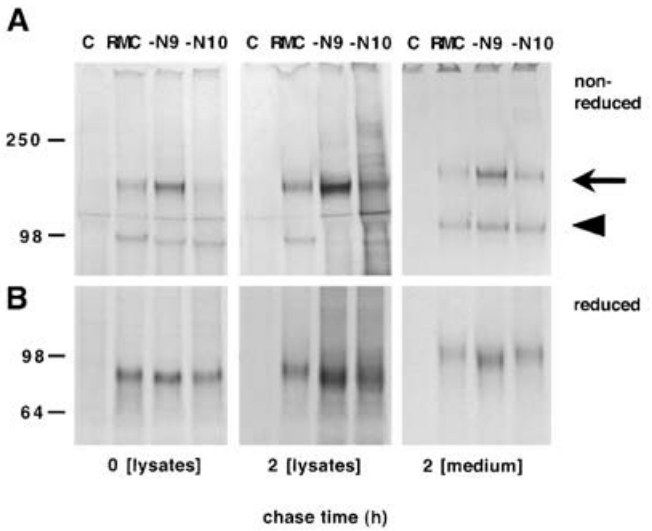

Figure 2 Alterations in dimer formation by mutant RMC-N9A

COS-1 cells were transfected with pSVL (vector control, C), pRMC, pRMC-N9A (-N9) and pRMC-N10A (-N10) constructs, pulsed for 15 min with ^{35}S Pro-mix, and products collected after 0 and 2 h chase periods by immunoprecipitation with anti-D4553 antibody. Lysates and medium were subjected to SDS/PAGE on 4–12 % gels after boiling for 3 min in the absence (**A**) or presence (**B**) of 10 mM dithiothreitol. Molecular-mass markers (kDa) are shown on the left. The arrow indicates the position of dimer species and the arrowhead marks monomers.

Mutations of asparagine to alanine at N-glycosylation positions N9 or N10 gave rise to dimers and monomers having mobilities that were fractionally faster than those of the wild-type RMC (Figure 2). This observation is consistent with the loss of one N-glycan chain in the product of each mutant. The most striking finding, however, was that mutation of the N9 consensus site resulted in a more intense dimer and, by 2 h, a less intense monomer than others. The decrease of monomer over time was not due to premature secretion, as no N-glycan mutant products appeared in the medium until 2 h (results not shown). The prominent dimer of RMC-N9A became even more pronounced after 2 h. Mutation of the N10 site, on the other hand, produced the same or slightly lower-intensity dimers than RMC at both 0 and 2 h of chase. This overall pattern of products was reproducible in more than seven independent transfections. As shown in Table 1 for the 0 and 2 h chase periods, the dimers of RMC-N9A constituted 91.8 % of the total lysate immunospecific radioactivity, whereas the comparable values for RMC and RMC-N10A were 75 and 70.6 % respectively. The difference between RMC and RMC-N9A was statistically highly significant ($P < 0.0001$). Products of the double mutant pRMC-N9A/N10A gave values that were only slightly less pronounced than those of RMC-N9A alone, whereas pRMC-N10A behaved like RMC. Thus dimer formation was favoured strongly in the absence of the N9 glycan.

Once secretion occurred, however, the high dimer/monomer ratio exhibited by RMC-N9A was not preserved. In medium samples the ratio was much lower than in cell lysates (2.4 compared with 17.2, Table 1), alerting us to the possibility that secretion

Table 1 Distribution (%) of labelled translation products of RMC, RMC-N9A and RMC-N10A between dimer and monomer during expression in COS-1 cells

Dimer and monomer are expressed as a percentage of total incorporated ^{35}S in immunoprecipitates (with total range of values or ± S.E.M. in parentheses) at 0 or 2 h of chase; *n* indicates the number of independent transfections. Student's *t* test (two-tailed, unpaired) indicated a significant difference between RMC and RMC-N9A dimers (lysates, $P < 0.0001$; medium, $P < 0.02$), but not between RMC and RMC-N10A (lysates, $P = 0.1232$; medium, $P = 0.2508$) after a 2 h chase period. D/M is the average dimer/monomer ratio.

	Total incorporated ^{35}S (%)							
	0 h Chase				2 h Chase			
	Dimer	Monomer	D/M	*n*	Dimer	Monomer	D/M	*n*
Lysates								
RMC	75.0 (61.8–83.0)	25.0 (17.0–38.2)	3.0	3	71.8 (±1.3)	28.2 (±1.3)	2.5	8
RMC-N9A	91.8 (85.9–95.6)	8.2 (4.4–14.1)	11.2	3	94.5 (±1.0)	5.5 (±1.0)	17.2	10
RMC-N10A	70.6 (61.5–87.0)	29.5 (13.0–38.5)	2.4	3	64.9 (±4.0)	35.1 (±4.0)	1.8	8
Medium								
RMC	0	0	0	3	54.2 (±4.5)	45.8 (±4.5)	1.2	7
RMC-N9A	0	0	0	3	70.3 (±3.9)	29.7 (±3.9)	2.4	9
RMC-N10A	0	0	0	3	61.5 (±4.0)	38.5 (±4.0)	1.6	7

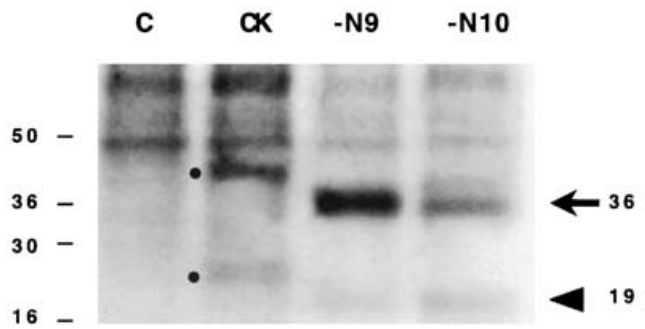

Figure 3 Expression of the CK domain and N9 and N10 mutants

COS-1 cells were transfected with vector control C, pCK, pCK-N9A and pCK-N10A. Pulse–chase studies were performed as described in the legend to Figure 2. The results reflect a 1-h chase. Lysates are shown after immunoprecipitation with anti-D4553 antibody and SDS/PAGE on a 4–20 % gel under non-reducing conditions. Filled circles (●) show the dimer and monomer of CK-expressing cells (45 and 22 kDa respectively). The arrow indicates dimer (36 kDa) species and the arrowhead marks monomers (19 kDa) in the CK-N9A and CK-N10A mutants.

and/or degradation of dimeric product may differ between these constructs. Later experiments addressed this issue.

Incorporation of radioactivity into the products of pCK, pCK-N9A and pCK-N10A

It was not possible to judge if the N9 and N10 mutations in RMC exerted their effects directly on the CK, or through more remote interactions with other regions of RMC. A shorter pCK construct was therefore synthesized and expressed in COS cells to examine the CK more directly. pCK is an N-terminally truncated version of RMC, consisting almost entirely of the CK motif (Figure 1). The only N-glycan sites present are those equivalent to N9 and N10 in RMC. The radioactive product of the pCK construct, which encodes fewer cysteine residues than pRMC, was more difficult to detect on autoradiographs. However, with longer exposure times (3–5 days) it was clear that pCK expressed a dimer (mid-point 45 kDa) and a monomer (mid-point 22 kDa; Figure 3). Both mutants pCK-N9A and pCK-N10A also formed dimers and monomers (36 and 19 kDa respectively). The ratio of dimer to monomer in CK-N9A (8.7) was greater than in either CK (2.1) or CK-N10 (2.9; an average of three transfections), which is qualitatively similar to the lysate findings seen above with RMC mutants. It was therefore concluded that N9 mutation exerts dimerization effects directly on the CK.

Possible causes of prominent RMC-N9A dimers

Theoretically, the increased intensity of the RMC-N9A (and pCK-N9A) dimers could arise from several causes. Possibilities such as differential transfection efficiency or differential effects on COS cell viability of the N9A and N10A mutants were considered highly unlikely. Mutation of asparagine to alanine changed only two nucleotides out of several thousand, which would not be expected to cause differential transfection efficiency. There were also no measurable differences among the three expressed RMC constructs in total cell lysate or medium protein, cell morphology or Trypan Blue exclusion (> 80 %; results not shown). More likely explanations that were considered included differences in post-translational events, such as more rapid dimerization of monomers of RMC-N9A, diminished secretion (retention) of RMC-N9A dimers and/or decreased degradation (increased stability) of RMC-N9A dimers. These possibilities were examined in subsequent experiments.

Formation of dimers

Kinetic studies were carried out using a short (5-min) pulse time to examine the early events of RMC product synthesis (Figure 4). At zero chase time, incorporation was minimal in all of the construct products. However, incorporation into dimers increased progressively over the next 30 min and was most marked in RMC-N9A (1.7-fold greater than in RMC), whereas RMC-N10A showed the same or slightly less incorporated radioactivity than RMC. During this period, a faint monomer band appeared for RMC and RMC-N10A, but no monomer was detected for RMC-N9A (results not shown), suggesting that initial dimerization in RMC-N9A may occur too rapidly for the precursor monomer to accumulate during the 5 min pulse period. The greater rate of incorporation of radioactivity into RMC-N9A dimers, coupled with the earlier finding of fewer monomers produced from this mutant, suggest that the dimer is synthesized more rapidly in RMC-N9A than in either RMC or RMC-N10A products. Whether the RMC-N9A dimer has the same structural integrity as RMC or RMC-N10A dimers was addressed in later experiments.

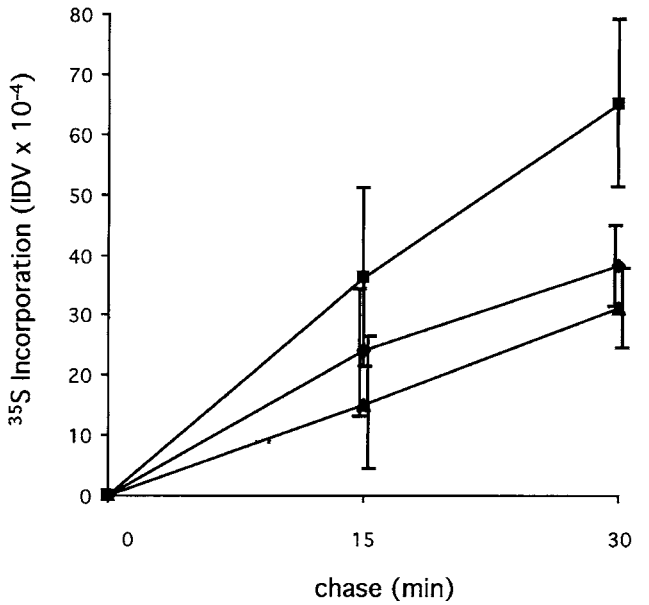

Figure 4 Kinetic study of incorporation of ^{35}S into pRMC, pRMC-N9A and pRMC dimers

Mean values of three independent experiments showing incorporated ^{35}S into dimers as detected in anti-D4553 immunoprecipitates of cell lysates after a 5-min pulse and chase periods as marked. ◆, RMC; ■, RMC-N9A (top); ▲, RMC-N10A (bottom). Vertical lines show 95 % confidence limits. IDV, integrated density values.

Secretory competence

To investigate the possibility that mutation of N9 results in less efficient secretion, RMC mutants were compared by measuring the percentage of total labelled mucin products (in cell lysates plus medium) that was secreted into the medium. In transfection experiments for all three mutants ($n = 7$–9), the product in the medium at 2 h was proportionately the same, about 34–38 % of the total labelled mucin ($P > 0.5$ when compared between all construct products). Thus an overall deficiency of secretion does not explain the increased intensity of RMC-N9A products observed in cell lysates. As noted earlier, however, the distribution of label between dimers and monomers differed between lysates and media samples for the RMC-N9A construct (Table 1). The difference suggests that there was more dissociation of dimer to monomer after the RMC-N9A dimers were secreted. If so, the enhancement of RMC-N9A dimerization in the ER is nullified after secretion because the RMC-N9A dimers are unstable.

Stability of cell dimers

The ER-located chaperone calreticulin has been shown in earlier studies to bind to precursors of human MUC2 [37], indicating that this chaperone normally assists in the folding of full-length mucin monomers to form stable dimers. Calreticulin was also found to bind to RMC. The antibody to calreticulin was used to immunoprecipitate cell products from all three constructs. After a 15 min radioactive pulse and zero chase time, monomers (and, more weakly, dimers) of all three constructs were detected (Figure 5). Over the next 60 min the chaperone was released gradually from all translation products, but of particular interest was the higher and more prolonged association of calreticulin with the dimers of RMC-N9A. RMC-N9A/N10A dimers gave a similar result with calreticulin (results not shown). The delay of calreticulin release suggests that these dimers were recognized

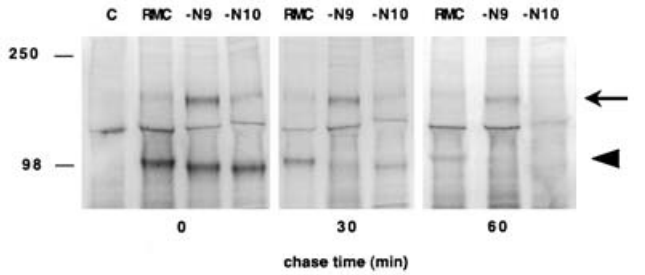

Figure 5 Immunoprecipitation of RMC, RMC-N9A and RMC-N10A with anti-calreticulin antibody

COS-1 cells were transfected as described in the legend of Figure 2, pulsed for 15 min and chased for periods as indicated. Lysates are shown after immunoprecipitation with anti-calreticulin antibody and SDS/PAGE on 4–12 % gels under non-reducing conditions. The arrow indicates dimers and the arrowhead indicates monomers. C indicates controls transfected with vector alone. Molecular-mass markers (kDa) are shown at the left.

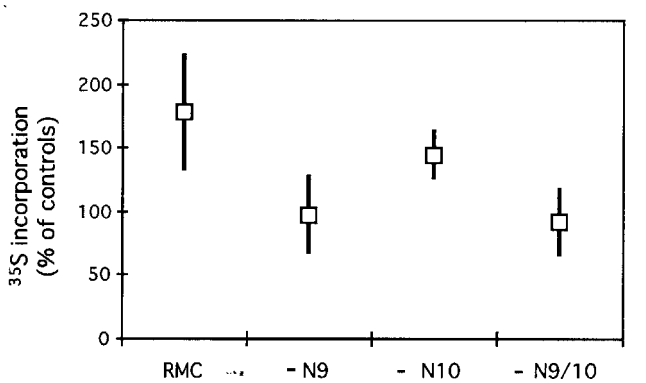

Figure 6 Inhibition of proteasomal degradation of RMC, RMC-N9A, RMC-N10A or RMC-N9A/N10A after treatment with clasto-lactacystin β-lactone

COS-1 cells were transfected and pulse labelled as described in the legend to Figure 2. DMSO (controls) or DMSO plus 10 μM β-lactone were added 60 min before the pulse, and during the 15 min pulse and 2 h chase. Lysates were immunoprecipitated with anti-D4553 antibody and subjected to SDS/PAGE on a 4–12 % gel under non-reducing conditions. Integrated density values ('IDV') of combined dimers plus monomers were expressed as a percentage of DMSO controls set to 100 %, and the means for each construct shown as boxes. Vertical line denote 95 % confidence limits.

as non-native or misfolded relative to the others, and were retained temporarily for further recycling through the quality-control system of the cell [27].

Proteasomal degradation

A proteasomal peptidase inhibitor, clasto-lactacystin β-lactone, the activated form of lactacystin [40,41], was suspended in DMSO, added to transfected cells 60 min prior to pulse labelling and was maintained throughout the 15 min pulse and 2 h chase periods. An equivalent volume of DMSO alone was added to duplicate transfections as controls. Figure 6 shows that RMC and RMC-N10A increased above control levels in lysates by approx. 75 and 45 % respectively after proteasomal inhibition, but no significant increases in RMC-N9A or RMC-N9/10A were detected. The confidence limits for RMC do not overlap with either RMC-N9A or RMC-N9/10A. These findings suggest that a portion of the N9-containing products (RMC and RMC-N10A) is normally degraded in proteasomes within 2 h of synthesis. Constructs lacking the N9 glycan, however, are not degraded

in proteasomes but are retained in the ER by calreticulin. This interpretation is consistent with the greater prominence of the RMC-N9A dimers observed above in cell lysates.

DISCUSSION

To our knowledge this study is the first demonstration that a single N-linked oligosaccharide may influence disulphide-dependent dimer formation of a mucin. Our findings do not of course rule out the possibility that one or more of the other eight N-glycans of RMC could exert independent effects on this process. They do suggest, however, that the N-glycan placement near a critical area of folding (ie. near Cys-1 and Cys-2 of the CK) may have an important conserved function. Mutation of the N10 glycan site did not produce major changes in synthesis, maturation or secretion of the RMC domain. In contrast, mutation of the N9 glycan site caused dimer formation in the ER to be more rapid, and dimers to remain more prominent than normal. Enhancement of dimer formation occurred regardless of potential contributions by any other N-glycans in RMC, since mutation of the N9 site in the shorter pCK construct, which contains the N9 and N10 sites only, also increased dimer formation.

The RMC-N9A mutation was not detrimental to overall secretion rates for RMC. However, the relative concentrations of labelled dimers and monomers differed in secretions versus cell lysates for the N9 mutant. In particular, there was a major decrease in the ratio of dimers to monomers in the media. Since there was no premature secretion of RMC-N9A monomers, and few monomers were detected in cell lysates at any time, it is likely that the loss of the N9 glycan led initially to accelerated but faulty subunit assembly into dimers. These products remained in dimeric form within cells, but after secretion most dissociated into monomers, even in the absence of reducing agents. Thus the prematurely formed dimers may be held together by random (unstable) disulphide or other weak interactions that do not survive well once diluted in the secretion media.

The dimers of RMC-N9A were not degraded in proteasomes during the 2 h of experimental observation, since inhibition of proteasomal enzymes by β-lactone did not cause further accumulation of RMC-N9A dimers. At least some of the faulty RMC-N9A dimers appear to have been retained in the ER, as reflected by their abnormally high concentration in cell lysates and their prolonged binding to calreticulin. This retention is consistent with the notion that the assembled dimers were misfolded or misaligned, thus recognized as non-native by the quality-control system of the cells.

Extended calreticulin binding also occurred in the RMC-N9A/N10A mutant. Calreticulin binding is reported to depend upon deglucosylation/reglucosylation of particular N-glycans by the folding sensor UDP-glucose/glycoprotein glucosyltransferase [42]. In the absence of both N9 and N10 glycans it is clear that calreticulin binding and the folding sensor must act on other moieties, perhaps glucose residues of one or more of the other N-glycans of RMC. Theoretically any of eight other N-glycans in RMC could serve in this capacity. Calreticulin binding studies were attempted on CK, CK-N9A and CK-N10A products to test chaperone interaction in the absence of the other eight N-glycans. Unfortunately calreticulin-labelled CK products in the immunoprecipitates were impossible to discern with confidence, given the large population of other calreticulin-bound proteins having the same size on gels (S. L. Bell, G. Xu, I. A. Khatri, R. Wang, S. Rahman and J. F. Forstner, unpublished work). Whether calreticulin bound to other N-glycans or to the RMC protein core itself [43] cannot, therefore, be answered at this time.

Our cumulative results are interpreted as indicating that the N9 glycan has a critical role in mucin biosynthesis, which is to slow the rate of formation of dimers. This delaying action probably permits sufficient time for the disulphide rearrangements that are needed to assemble stable dimers that maintain their structural stability even after secretion. The mechanism by which the N9-glycan counterbalances the otherwise excessively rapid folding and/or assembly process is uncertain, although some precedents for this action have been recognized. For example, in a study of the insulin receptor, Bass and colleagues [44] showed that N-linked glycans and their interaction with the chaperones calnexin and calreticulin delayed dimer formation, but facilitated correct folding and transport competency of the peptide. In other examples, both accelerated and decelerated rates of folding were observed in association with specific N-glycan site mutations of influenza haemagglutinin [45]. It is possible that the N9 oligosaccharide alters the ionic or electrostatic microenvironment of the RMC polypeptide to reduce exposure of nearby thiol groups to solvent [46], and thereby retard dimer formation.

Physical techniques have been useful in showing that attachment of oligosaccharides to their peptide substrates sometimes exerts profound local conformational effects, with subsequent functional consequences on secondary processes such as chaperone binding, solubility, protein aggregation, receptor binding and secretory transport (reviewed by [23,25]). Wormald et al. [29,30] have reviewed NMR, molecular modelling and crystallographic data for a number of peptides, and have concluded that linkages between asparagine of peptides and core N-glycan carbohydrates are usually fairly rigid and planar. This decrease in flexibility constrains the number of peptide conformations that can be adopted, and is due to steric, hydrophobic and/or hydrophilic interactions between the core glycan residues and neighbouring amino-acid side chains. In consequence there is reduced fluctuation and increased thermostability of tertiary or quaternary folding of the protein.

There are also conformational influences on proteins bearing O-linked oligosaccharides, including mucins. Closely spaced clusters of O-glycans maintain an extended linear configuration of the apomucin core [47–49]. In a recent study Satyanarayana et al. [50] examined a 23-residue MUC7 peptide using CD spectroscopy, NMR and molecular-dynamics simulation, and demonstrated that the apopeptide was mainly in a β-strand conformation, whereas the glycosylated counterpart adopted a partially helical structure. The transition was due to a hydrogen-bonded salt bridge between an O-glycan chain hydroxyl group and a lysine side chain. Once in a helical configuration, the glycopeptide exhibited a greater tendency to undergo hydrophobic interactions and self-association.

Interesting relationships between N-glycosylation, disulphide-dependent folding and dimer stability have been established for the pituitary glycoprotein hormone family of CK-containing proteins. Human chorionic gonadotropin (hCG), like the other members of this family, consists of a heterodimer of CK-containing α and β subunits. Feng et al. [51] showed that the two N-linked oligosaccharides of the β subunit of hCG are required for optimal folding kinetics of the CK of the β subunit. Interestingly, co-expression of a normal α subunit and a slowly folding mutant β subunit restored β subunit folding rates and provided stability to the $\alpha\beta$ heterodimer. An N-glycan at Asn-52 of the α subunit (αAsn-52), in close proximity to the first cysteine of the CK, was shown to be critical for this function [52]. Crystallography of hCG showed that the N-glycan on αAsn-52 forms intersubunit hydrophobic contacts with five amino acids at the interface with the β subunit [14]. Crystallography of human follicle-stimulating hormone (hFSH), another pituitary glycoprotein hormone which

also forms $\alpha\beta$ heterodimers, showed that the N-glycan on αAsn-52 forms a hydrogen bond with Tyr-58 of the β subunit [19], which is probably the mechanism responsible for stabilization of the dimer.

There have been no physical studies probing the mechanism by which the N9-glycan of RMC slows homodimer formation, but the gonadotropin observations above suggest that an interaction between RMC monomers mediated by the N9 glycan could be considered. For example, the N9 glycan in each monomer may provide a 'spacer', keeping the monomers separated until their CK folding matures to the stage that stable disulphide-bonded dimers can be formed. The use of a single N-glycan on each monomer as a 'spacer' or 'separator' of monomers has been seen in the case of IgG Fc chains [53]. The 'open' spacing between the Cγ2 domains in Fc homodimers is maintained by a single N-glycan present in each Fc peptide. Progressive truncation of the oligosaccharide shifted the open configuration to a more 'closed' one, which is known to cause decreased binding of the Cγ2 dimer to its Fc receptor. By analogy, in our mutant RMC-N9A multiple alternative conformations may be possible, causing dimers to form more rapidly than normal. The dimers may not be as stable or transport-competent as native dimers, however. In the presence of the N9 glycan mature dimers form, after which the need for the N9 glycan disappears. This hypothesis is consistent with earlier observations that exposure of mature RMC dimers to N-glycosidase F removes sugars but does not alter dimer stability [21].

Our results with RMC imply that the longer-term functional effects of N9 glycan site mutation would be continuous formation of incorrectly assembled dimers, slower than normal intracellular transport of the dimers (partial ER retention), coupled with secretion of an unstable mucin that readily dissociates and loses its gel-forming properties. Prevention of N9 oligosaccharide synthesis would thus reduce gel formation and/or viscoelasticity of secreted mucin, and could be a specific target for therapy in which increased luminal mucolysis is a desired goal. Intestinal and/or pulmonary mucus obstruction, as seen in cystic fibrosis and other chronic obstructive diseases, represent examples of pathology that might benefit from this form of targeted mucolysis.

Financial support was provided by the Canadian Cystic Fibrosis Foundation, The Hospital for Sick Children, Toronto, and the Canadian Institutes of Health Research. We also thank Mr Fariborz Rashid-Kolvear (Cell Biology Program) and Dr Mary Corey (Population Health Sciences Program), at the Hospital for Sick Children, for helpful discussions and advice.

REFERENCES

1 Probst, J. C., Gertzen, E.-M. and Hoffmann, W. (1990) An integumentary mucin (FIM-B.1) from *Xenopus laevis* homologous with von Willebrand factor. Biochemistry **29**, 6240–6244
2 Eckhardt, A. E., Timpte, C. S., Abernethy, J. L., Zhao, Y. and Hill, R. L. (1991) Porcine submaxillary mucin contains a cystine-rich, carboxyl-terminal domain in addition to a highly repetitive, glycosylated domain. J. Biol. Chem. **266**, 9678–9686
3 Xu, G., Huan, L., Khatri, I., Sajjan, U. S., McCool, D., Wang, D., Jones, C., Forstner, G. and Forstner, J. (1992) Human intestinal mucin-like protein (MLP) is homologous with rat Mlp in the C-terminal region, and is encoded by a gene on chromosome 11 p 15.5. Biochem. Biophys. Res. Commun. **183**, 821–828
4 Meerzaman, D., Charles, P., Daskal, E., Polymeropoulos, M. H., Martin, B. M. and Rose, M. C. (1994) Cloning and analysis of cDNA encoding a major airway glycoprotein, human tracheobronchial mucin (MUC5). J. Biol. Chem. **269**, 12932–12939
5 Lesuffleur, T., Roche, F., Hill, A. S., Lacasa, M., Fox, M., Swallow, D. M., Zweibaum, A. and Real, F. X. (1995) Characterization of a mucin cDNA clone isolated from HT-29 mucus-secreting cells. J. Biol. Chem. **270**, 13665–13673
6 Desseyn, J.-L., Aubert, J.-P., Van Seuningen, I., Porchet, N. and Laine, A. (1997) Genomic organization of the 3′ region of the human mucin gene *MUC5B*. J. Biol. Chem. **272**, 16873–16883
7 Toribara, N. W., Ho, S. B., Gum, E., Gum, Jr, J. R., Lau, P. and Kim, Y. S. (1997) The carboxyl-terminal sequence of the human secretory mucin, MUC6. J. Biol. Chem. **272**, 16398–16403
8 Turner, B. S., Bhaskar, K. R., Hadzopoulou-Cladaras, M. and LaMont, J. T. (1999) Cysteine-rich regions of pig gastric mucin contain von Willebrand factor and cystine knot domains at the carboxyl terminal. Biochim. Biophys. Acta **1447**, 77–92
9 Vitt, U. A., Hsu, S. Y. and Hsueh, A. J. W. (2001) Evolution and classification of cystine knot-containing hormones and related extracellular signaling molecules. Mol. Endocrinol. **15**, 681–694
10 Craik, D. J., Daly, N. L. and Waine, C. (2001) The cystine knot motif in toxins and implications for drug design. Toxicon **39**, 43–60
11 McDonald, N. Q., Lapatto, R., Murray-Rust, J., Gunning, J., Wlodawer, A. and Blundell, T. L. (1991) New protein fold revealed by a 2.3-Å resolution crystal structure of nerve growth factor. Nature (London) **354**, 411–414
12 Oefner, C., D'Arcy, A., Winkler, F. K., Eggimann, B. and Hosang, M. (1992) Crystal structure of human platelet-derived growth factor BB. EMBO J. **11**, 3921–3926
13 Schlunegger, M. P. and Grütter, M. G. (1992) An unusual feature revealed by the crystal structure at 2.2 Å resolution of human transforming growth factor-β2. Nature (London) **358**, 430–434
14 Lapthorn, A. J., Harris, D. C., Littlejohn, A., Lustbader, J. W., Canfield, R. E., Machin, K. J., Morgan, F. J. and Isaacs, N. W. (1994) Crystal structure of human chorionic gonadotropin. Nature (London) **369**, 455–461
15 Muller, Y. A., Li, B., Christinger, H. W., Wells, J. A., Cunningham, B. C. and De Vos, A. M. (1994) Vascular endothelial growth factor: crystal structure and functional mapping of the kinase domain receptor binding site. Proc. Natl. Acad. Sci. U.S.A. **94**, 7192–7197
16 Muller, Y. A., Christinger, H. W., Keyt, B. A. and De Vos, A. M. (1997) The crystal structure of vascular endothelial growth factor (VEGF) refined to 1.93 Å resolution: multiple copy flexibility and receptor binding. Structure **5**, 1325–1338
17 Scheufler, C., Sebald, W. and Hulsmeyer, M. (1999) Crystal structure of human bone morphogenetic protein-2 at 2.7 Å resolution. J. Mol. Biol. **287**, 103–115
18 Hymowitz, S. G., Filvaroff, E. H., Yin, J., Lee, J., Cai, L., Risser, P., Maruoka, M., Mao, W., Foster, J., Kelley, R. F. et al. (2001) IL-17s adopt a cystine knot fold: structure and activity of a novel cytokine, IL-17F, and implications for receptor binding. EMBO J. **20**, 5332–5341
19 Fox, K. M., Dias, J. A. and Van Roey, P. (2001) Three-dimensional structure of human follicle-stimulating hormone. Mol. Endocrinol. **15**, 378–389
20 Bell, S. L., Xu, G. and Forstner, J. F. (2001) Role of the cystine knot motif at the C-terminus of rat Muc2 in dimer formation and secretion. Biochem. J. **357**, 203–209
21 Bell, S. L., Khatri, I. A., Xu, G. and Forstner, J. F. (1998) Evidence that a peptide corresponding to the rat Muc2 C-terminus undergoes disulphide-mediated dimerization. Eur. J. Biochem. **253**, 123–131
22 Kornfeld, R. and Kornfeld, S. (1985) Assembly of asparagine-linked oligosaccharides. Annu. Rev. Biochem. **54**, 631–664
23 Parodi, A. J. (2000) Role of N-oligosaccharide endoplasmic reticulum processing reactions in glycoprotein folding and degradation. Biochem. J. **348**, 1–13
24 Frigerio, L. and Lord, J. M. (2000) Glycoprotein degradation: do sugars hold the key? Curr. Biol. **10**, R674–R677
25 Helenius, A. and Aebi, M. (2001) Intracellular functions of N-linked glycans. Science **291**, 2364–2369
26 Lehrman, M. A. (2001) Oligosaccharide-based information in endoplasmic reticulum quality control and other biological systems. J. Biol. Chem. **276**, 8623–8626
27 Cabral, C. M., Liu, Y. and Sifers, R. N. (2001) Dissecting glycoprotein quality control in the secretory pathway. Trends Biochem. Sci. **26**, 619–624
28 Roth, J. (2002) Protein *N*-glycosylation along the secretory pathway: relationship to organelle topography and function, protein quality control, and cell interactions. Chem. Rev. **102**, 285–303
29 Wormald, M. R. and Dwek, R. A. (1999) Glycoproteins: glycan presentation and protein-fold stability. Structure **7**, R155–R160
30 Wormald, M. R., Petrescu, A. J., Pao, Y.-L., Glithero, A., Elliott, T. and Dwek, R. A. (2002) Conformational studies of oligosaccharides and glycopeptides: complementarity of NMR, X-ray crystallography, and molecular modelling. Chem. Rev. **102**, 371–386
31 Helenius, A. (1994) How N-linked oligosaccharides affect glycoprotein folding in the endoplasmic reticulum. Mol. Biol. Cell **5**, 253–265
32 Ellgaard, L., Molinari, M. and Helenius, A. (1999) Setting the standards: quality control in the secretory pathway. Science **286**, 1882–1888
33 Molinari, M. and Helenius, A. (2000) Chaperone selection during glycoprotein translocation into the endoplasmic reticulum. Science **288**, 331–333
34 Dekker, J. and Strous, G. J. (1990) Covalent oligomerization of rat gastric mucin occurs in the rough endoplasmic reticulum, is N-glycosylation-dependent, and precedes initial O-glycosylation. J. Biol. Chem. **265**, 18116–18122
35 McCool, D. J., Forstner, J. F. and Forstner, G. G. (1994) Synthesis and secretion of mucin by the human colonic tumour cell line LS180. Biochem. J. **302**, 111–118

36 van Klinken, B. J.-W., Einerhand, A. W. C., Büller, H. A. and Dekker, J. (1998) The oligomerization of a family of four genetically clustered human gastrointestinal mucins. Glycobiology **8**, 67–75
37 McCool, D. J., Okada, Y., Forstner, J. F. and Forstner, G. G. (1999) Roles of calreticulin and calnexin during mucin synthesis in LS180 and HT29/A1 human colonic adenocarcinoma cells. Biochem. J. **341**, 593–600
38 Xu, G., Huan, L.-J., Khatri, I. A., Wang, D., Bennick, A., Fahim, R. E., Forstner, G. G. and Forstner, J. F. (1992) cDNA for the carboxyl-terminal region of a rat intestinal mucin-like peptide. J. Biol. Chem. **267**, 5401–5407
39 Robbins, P. W., Trimble, R. B., Wirth, D. F., Hering, C., Maley, F., Maley, G. F., Das, R., Gibson, B. W., Royal, N. and Biemann, K. (1984) Primary structure of the *Streptomyces* enzyme endo-beta-N-acetylglucosaminidase H. J. Biol. Chem. **259**, 7577–7583
40 Dick, L. R., Cruikshank, A. A., Grenier, L., Melandri, F. D., Nunes, S. L. and Stein, R. L. (1996) Mechanistic studies on the inactivation of the proteasome by lactacystin. J. Biol. Chem. **271**, 7273–7276
41 Craiu, A., Gaczynska, M., Akopian, T., Gramm, C. F., Fenteany, G., Goldberg, A. L. and Rock, K. L. (1997) Lactacystin and clasto-lactacystin β-lactone modify multiple proteasome β-subunits and inhibit intracellular protein degradation and major histocompatibility complex class I antigen presentation. J. Biol. Chem. **272**, 13437–13445
42 Sousa, M. and Parodi, A. J. (1995) The molecular basis for the recognition of misfolded glycoproteins by the UDP-glc:glycoprotein glucosyltransferase. EMBO J. **14**, 4196–4203
43 Saito, Y., Ihara, Y., Leach, M. R., Cohen-Doyle, M. F. and Williams, D. B. (1999) Calreticulin functions *in vitro* as a molecular chaperone for both glycosylated and non-glycosylated proteins. EMBO J. **18**, 6718–6729
44 Bass, J., Chiu, G., Argon, Y. and Steiner, D. F. (1998) Folding of insulin receptor monomers is facilitated by the molecular chaperones calnexin and calreticulin and impaired by rapid dimerization. J. Cell Biol. **141**, 637–646
45 Hebert, D. N., Foellmer, B. and Helenius, A. (1996) Calnexin and calreticulin promote folding, delay oligomerization and suppress degradation of influenza hemagglutinin in microsomes. EMBO J. **15**, 2961–2968
46 Creighton, T. E. (1997) Protein folding coupled to disulphide bond formation. Biol. Chem. **378**, 731–744
47 Gerken, T. A., Butenhof, K. J. and Shogren, R. (1989) Effects of glycosylation on the conformation and dynamics of O-linked glycoproteins: carbon-13 NMR studies of ovine submaxillary mucin. Biochemistry **28**, 5536–5543
48 Shogren, R., Gerken, T. A. and Jentoft, N. (1989) Role of glycosylation on the conformation and chain dimensions of O-linked glycoproteins: light-scattering studies of ovine submaxillary mucin. Biochemistry **28**, 5525–5536
49 Schuman, J., Campbell, A. P., Koganty, R. R. and Longenecker, B. M. (2003) Probing the conformational and dynamical effects of O-glycosylation within the immunodominant region of a MUC1 peptide tumor antigen. J. Peptide Res. **61**, 91–108
50 Satyanarayana, J., Gururaja, T. L., Narasimhamurthy, S., Naganagowda, G. A. and Levine, M. J. (2001) Synthesis and conformational features of human salivary mucin C-terminal derived peptide epitope carrying Thomsen-Friedenreich antigen: Implications for its role in self-association. Biopolymers **58**, 500–510
51 Feng, W., Matzuk, M. M., Mountjoy, K., Bedows, E., Ruddon, R. W. and Boime, I. (1995) The asparagine-linked oligosaccharides of the human chorionic gonadotropin β subunit facilitate correct disulfide bond pairing. J. Biol. Chem. **270**, 11851–11859
52 Heikoop, J. C., Van den Boogaart, P., De Leeuw, R., Rose, U. M., Mulders, J. W. M. and Grootenhuis, P. D. J. (1998) Partially deglycosylated human choriogonadotropin, stabilized by intersubunit disulfide bonds, shows full bioactivity. FEBS Lett. **253**, 354–356
53 Krapp, S., Mimura, Y., Jefferis, R., Huber, R. and Sondermann, P. (2003) Structural analysis of human IgG-Fc glycoforms reveals a correlation between glycosylation and structural integrity. J. Mol. Biol. **325**, 979–989

Received 9 January 2003/16 April 2003; accepted 13 May 2003
Published as BJ Immediate Publication 13 May 2003, DOI 10.1042/BJ20030096